中國機械工程學刊第四十卷第六期第 693~701 頁(民國一百零八年)
Journal of the Chinese Society of Mechanical Engineers, Vol.40, No.6, pp 693~692 (2019)

Design and Control of a Novel Two Different Stiffness Series Elastic Actuator

Kai-Yang Yin*, Kui Xiang, Jing Chen** and Mu-Ye Pang*****

Key words: Series Elastic Actuator; Segmental control; Smooth switching control; Linear quadratic regulator

ABSTRACT

Series elastic actuators (SEA) are desirable for human-centered robotics. However, conventional series elastic actuators face a performance limitation due to the compromise on the elastic element stiffness selection. This paper presents a novel two different stiffness series elastic actuator (DSSEA) and an optimal controller for it to address the performance limitation. In particular, two both stiffness and length are different springs were chosen as the elastic element of the DSSEA. The low stiffness spring single used to deal with the low force operation and the two spring combined used to handle the large force operation. To address the challenge of the smooth transition between those two operation cases, a segmental model-based feedback controller with feedforward compensation is proposed, and a smooth switching controller is designed to handle the transition interval. The experimental results from DSSEA prototype demonstrate that the proposed controller can achieve excellent force tracking performance at both low, high, and wide-bound force range operation.

INTRODUCTION

In recent years, the human-centered robot has a booming of developing to support people to achieve different physical tasks, such as: such as assistive and rehabilitation robots, service robots (Boccanfuso et al. 2017, Kui etal. 2015). In these applications, the robot requires direct interaction with human beings. As a result, human-centered robotics systems must consider the human's safety and comfort (Tadele et al. 2014). This motivates the research of compliant actuators (CA) which have the ability of safety interact with the user and can provide compliant force. Series elastic actuator (SEA) as one of the well-known CA was first proposed in the work of (Pratt et al. 1995). In SEA, an elastic element which is placed between the motor-gearbox and the load make compliance action force to be possible.

Many different SEA has been designed for a human-centered robot. In (Orekhov et al. 2015), a SEA is developed based on a linear spring coupled to a roller screw. In (Baldoni et al. 2018), a rotary SEA is designed based on a Bowden cable is connected to linear spring. The performance of SEA largely depends on the stiffness coefficient of the elastic element (Roozing et al. 2017). Low stiffness elastic element produces high fidelity of force control, low output impedance, and reduces friction, but also limits the force range. High stiffness elastic element increases operation peak force but reduces force control fidelity and output impedance. The compromise between the range of operation force and performance of the actuator has to be reached due to the selection of the spring stiffness. To overcome this trade-off, most current SEA are designed with variable stiffness springs, leading to a complex control system and bulky physical design (Wolf et al. 2016).

We get the idea of designing a novel two different stiffness series elastic actuator (DSSEA) form the soft tissues of human and other animals. In a long period of natural evolution, human and other animals can adapt to various complex environments, and the soft tissues have significantly shock-proof. In the human body, soft tissues are the organization that strengthens stiffness. When the load increase, the corresponding stiffness will also increase. The maximal stiffness to minimal stiffness of soft tissues is about 5 times (Li et al. 2004). This stiffness characteristic of human soft tissue makes joint movement excellent flexibility and adaptability. According to this insight, DSSEA is designed to overcome the performance limit of the traditional

Paper Received May, 2019. Revised July, 2019. Accepted December, 2019.Author for Correspondence:Kui Xiang

PhD Candidate, School of Automation, Wuhan University of Technology, Wuhan 430070, P.R. China and lecturer, School of Electrical and Mechanical Engineering, Pingdingshan University, Pingdingshan 467000, China

***Professor, School of Automation, Wuhan University of Technology, Wuhan 430070, China.*

**** Associate Professor, School of Automation, Wuhan University of Technology, Wuhan 430070, China.*

SEA. One of the novelties is used soft and stiff springs parallel as the elastic element of the actuator. The low stiffness spring single used to deal with the low force operation to ensure high force fidelity and the two spring combined used to handle the large force operation to achieve large peak force.

Apart from the mechanical improvement of SEAs, the control strategy is also gaining attention in recent years. In (Paine et al. 2014, Yin et al. 2018), pure PID controller is used to producing the desired force. In (Roozing et al. 2016), PID plus disturbance observer is presented to improve the dynamical performance of SEAs. In (Vallery et al. 2008), a type of cascaded control is designed to generate desired force and low impedance. In (Kong et al. 2009, Yin et al. 2018), optimal feedback plus feedforward controller is proposed. However, all this control strategy is not very suitable for the DSSEA, as the different stiffness spring worked in different force ranges. One challenge of the control system is to make a smooth transition between low and high force ranges. To address the challenge of the smooth transition between those two operation cases, a segmental model-based feedback controller with feedforward compensation is proposed, and a smooth switching controller is designed to handle the transition interval.

The rest of this paper is organized as follows. First, two dynamical models are established for low force range and high force range. Second, segmental model-based feedback with feedforward compensation controller and a smooth switching control are proposed. Third, introduces the experimental results demonstrating its force control performance. In the end, a brief discussion and conclusion are given.

DSSEA DESIGN

In this section, we describe the hardware and the model of the NSSEA.

Hardware of NSSEA

The basic idea in NSSEA is utilized two linear spring as the elastic element to overcome the major limitations in the existing conventional SEA design. Fig. 1 shows the CAD model of the NSSEA. It consists of a servomotor with a rotary encoder, a pair of synchromesh gear with appropriate gear ratio to transmit the motion to the ball screw, a ball screw converts the shaft rotary motion to the nut linear motion, two linear springs attached to the ball screw nut and transmit the force to the output limb which is used to transmit the operation force to the load, and a linear encoder (2000 counts/in.) measures the compression of the spring. The actuator force is easily obtained by measuring the spring deflection and be used as the feedback for the force control which is detailed in the next section.

Fig. 2 shows the NSSEA prototype built based on the above design. The NSSEA is designed to be able to provide up to 150N output force. A Maxon DC brushless motor (RE40) is used due to its lightweight and high power density. Lightweight motor prevents over-burdening the actuator structure with excess mass. The ball screw has a pitch of 3mm/rev and a length of 183mm. The low stiffness linear spring have spring constant of 7.55N/mm and the alone working stroke of 10mm. It can provide an output force of 75.5N and used to operate in the range of about 50% of the full force. The large stiffness linear spring have spring constant of 60.63N/mm. The two linear spring parallel working stroke is 1.1mm. The total mass of the novel actuator is 1.41kg.

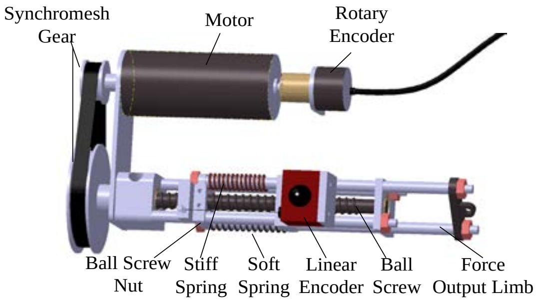

Figure 1. CAD model of the NSSEA.

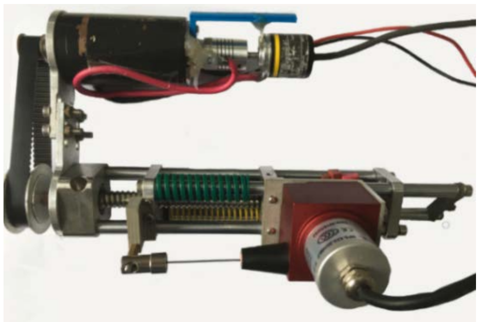

Figure 2. The prototype of the NSSEA.

Table 1. Parameter of the NSSEA.

Symbol	Quantity	Value
m_m	Motor equivalent mass	11Kg
bm	Motor & ball screw damping	2200Ns/m
F_{max}	Max output force	150N
k_1	Low stiffness spring constant	7.55×10^3 N/m
k_2	Larger stiffness spring constant	60.63×10^3 N/m
l_1	Low stiffness spring alone stroke	1×10^{-2}m
l_2	Both spring parallel stroke	1.1×10^{-3}m
L	Ball screw length	183m
I	Ball screw Pitch	3×10^{-3}m
M	Actuator total weight	1.41kg

Model of NSSEA

In this section, a basic model of novel SEA will be proposed, which contain the essential elements of the actuator. To analyze the NSSEA performance at the output end, the actuator is modeled consists of only transmission devices. It converts the rotary elements to equivalent translational elements and satisfying Eq. (1).

$$F_m = \frac{T_r 2\pi\rho}{I}, \tag{1}$$

where F_m is the motor equal input force, T_r represents the motor input torque, I refer to the pitch of the ball screw, ρ=91% implies the transmission efficiency.

The model for equivalent translational motion is shown in Fig.3. In those models, F_l implies the force output which is measured by the deflection of the spring, m_m represents the equivalent mass of motor as derived in Eq. (2), b_m is the viscous damping for motor and ball screw, x_l refers to the relative position of the load, x_m represents the relative position of the ball screw nut, k_1 is the spring constant of low stiff spring, k_2 is the spring constant of larger stiff spring. The physical parameters of the novel SEA are listed in Table. 1. When the NSSEA working in the low force range (0~75N), the NSSEA behave like a normal SEA with the low stiffness spring is single action as shown in Fig. 3(a). However, when the NSSEA working in the high force range (75~150N), it also behaves like a normal SEA and the force control is based on the parallel of the two linear spring as shown in Fig. 3.(b).

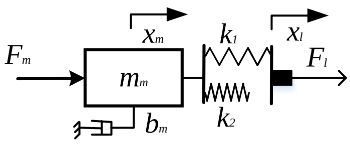

(a) Model of low force range.

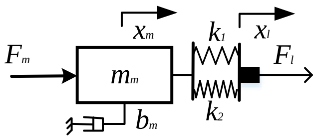

(b) Model of high force range

Figure 3. Translation motion model of NSSEA.

$$m_m = J_1\left(\frac{2\pi}{I}\right)^2, \tag{2}$$

where J_1 refers to the moment of inertia of the motor, mm represents the mass of ball screw nut.

Model of low force range

When the NSSEA working in the low force range, the equivalent translational elements can be seen as two degrees of freedom system. Referring to Fig. 3(a), the constitutive equations of motion according to Newton's second law are defined by the force in the spring and motion of the equivalent motor mass.

$$\begin{cases} F_{m1} - m_m\ddot{x}_m - b_m\dot{x}_m - F_{l1} = 0 \\ F_{l1} = k_1(x_m - x_l) \end{cases}, \tag{3}$$

where F_{m1} is the motor input force in low force range, F_{l1} refers to the output force in low force range. Assuming the load end is fixed, x_l=0, we can get:

$$\ddot{F}_{l1} = \frac{k_1}{m_m}F_{m1} - \frac{k_1}{m_m}F_{l1} - \frac{b_m}{m_m}\dot{F}_{l1}. \tag{4}$$

However, Eq. (3) does not consider the effects of frictional force. Thus, a complete model with frictional compensation of low force range should be:

$$\ddot{F}_{l1} = \frac{k_1}{m_m}F_{m1} - \frac{k_1}{m_m}F_{l1} - \frac{b_m}{m_m}\dot{F}_{l1} + \Delta f\left(\dot{x}_m\right), \tag{5}$$

where $\Delta f(\dot{x}_m)$ refers to frictional compensation item, can be written as:

$$\Delta f(\dot{x}_m) = \mu\,\mathrm{sgn}\left(\dot{x}_m\right), \tag{6}$$

where μ can be estimated with a basic experiment. The experimental results of the open-loop slope response for the NSSEA prototype are shown in Fig. 4. When the input force greater than 40N, the output force increase with the rise of the input force. At the peak force 72N, the output force is 30N. Form the experimental results, it can be estimated that μ is about 42N.

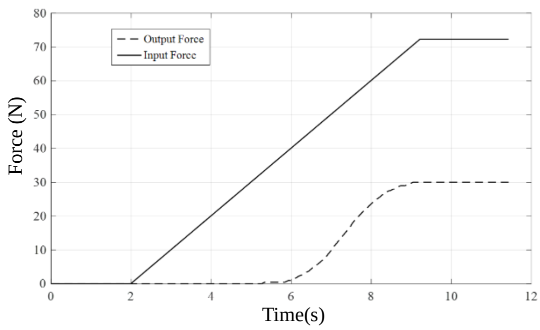

Figure 4. Open-loop slope response for the NSSEA prototype.

Model of high force range

Referring to Fig.3 (b), the constitutive equations for high force range can be written as:

$$\begin{cases} F_{m2} - m_m\ddot{x}_m - b_m\dot{x}_m - F_{l2} = 0 \\ F_{l2} = \left(k_1 + k_2\right)\left(x_m - \Delta x - x_l\right) + k_1\Delta x \end{cases}, \tag{7}$$

where Δx=10mm refers to the maximum displacement of low stiffness spring alone working. F_{m2} is the motor input force in high force range, F_{l2} refers to the output force in high force range. Assuming the load end is fixed, x_l=0, we can get:

$$\ddot{F}_{l2} = \frac{k_1 + k_2}{m_m} F_{m2} - \frac{k_1 + k_2}{m_m} F_{l2} - \frac{b_m}{m_m} \dot{F}_{l2} . \tag{8}$$

However, Eq. (8) does not consider the effects of frictional force. Thus, a complete model with frictional compensation of high force range should be:

$$\ddot{F}_{l2} = \frac{k_1 + k_2}{m_m} F_{m2} - \frac{k_1 + k_2}{m_m} F_{l2} - \frac{b_m}{m_m} \dot{F}_{l2} + \Delta f\left(\dot{x}_m\right) . \tag{9}$$

CONTROLLER DESIGN

Segmental model-based feedback with feedforward compensation controller and a smooth switching controller are proposed for the NSSEA. As the actuator has piecewise linear spring constant at different force ranges, it needs to switch the controller between the different control designs for the two operation force ranges. During the switch, the smooth switching control is designed to make a smooth transition between low force range and high force range. The torque control loop is used as a motor controller which can overcome some undesirable effects of the motor and the gearbox. The torque control of the motor is very mature, and thus the details are omitted here. This paper mainly introduces the design of outer-loop feedback control. Fig.5 shows the controller structure for the NSSEA.

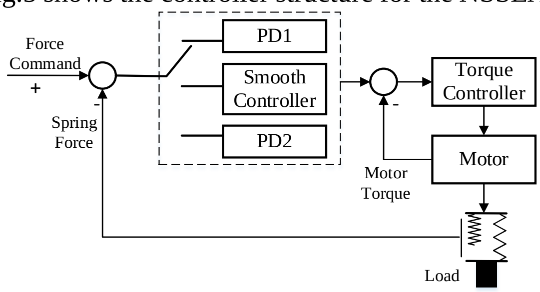

Figure 5. Controller structure of the NSSEA.

Low force control

Model-Based feedback control for low operation force range is designed. The force error is defined as $e_1 = F_{d1}(t) - F_{l1}(t)$, and the derivative force error is given by $\dot{e}_1 = \dot{F}_{d1}(t) - \dot{F}_{l1}(t)$. F_{d1} refers to the desired force. Define the state matrix $E_1 = [e_1, \dot{e}_1]^T$, then the state equation can be written as:

$$\dot{E}_1 = \begin{bmatrix} \dot{e}_1 \\ \ddot{e}_1 \end{bmatrix} = A_1 E_1 - B_1 F_{m1} + B_1 \left[\frac{m_m}{k_1} \ddot{F}_{d1} + \dot{F}_{d1} + \frac{b}{k_1} F_{d1} - \frac{m_m}{k_1} \Delta f(\dot{x}_m) \right] , \tag{10}$$

where

$$A_1 = \begin{bmatrix} 0 & 1 \\ -\frac{k_1}{m_m} & -\frac{b}{m_m} \end{bmatrix}, \quad B_1 = \begin{bmatrix} 0 \\ \frac{k_1}{m_m} \end{bmatrix} . \tag{11}$$

The proportional derivative (PD) controller should be designed. The control law can be written as:

$$u_1(t) = K_{p1} e_1 + K_{d1} \dot{e}_1 , \tag{12}$$

where K_{p1}、K_{d1} are the appropriate gain parameters. Simplified the Eq. (10), we have the following linear model:

$$\dot{E}_1 = \begin{bmatrix} \dot{e}_1 \\ \ddot{e}_1 \end{bmatrix} = A_1 E_1 - B_1 F_{m1} , \tag{13}$$

Let

$$F_{m1} = c u_1(t) , \tag{14}$$

where c represents torque constant of motor, From Eq. (10)~(14) the linear model can be written as:

$$\dot{E}_1 = \begin{bmatrix} 0 & 1 \\ -\frac{k_1}{m_m} - \frac{ck_1}{m_m} K_{p1} & -\frac{b}{m_m} - \frac{ck_1}{m_m} K_{d1} \end{bmatrix} E_1 . \tag{15}$$

Therefore, the characteristic equation of the closed-loop system is:

$$s^2 + \left(\frac{b}{m_m} + \frac{ck_1}{m_m} K_{d1} \right) s + \frac{k_1}{m_m} + \frac{ck_1}{m_m} K_{p1} = 0 . \tag{16}$$

We apply the Linear Quadratic Regulator (LQR) design theory to optimize gain parameters. The performance index of optimal control is introduced, an input u_1 is designed to that:

$$J_1 = \int_0^\infty (E_1^T Q_1 E_1 + \rho_1 u_1^2) dt , \tag{17}$$

where Q_1 is a symmetric positive-definite matrix and refers to the weighting matrix for E_1, ρ_1 is a positive constant. According to the LQR optimal control theory (Kwakernaak et al. 1972), if the J_1 minimize, the feedback control law should be:

$$u_1(t) = \rho_1^{-1} B_1^T P_1 E_1(t) , \tag{18}$$

where P_1 is a unique positive definite matrix and satisfies the famous Riccati differential equations:

$$A_1^T P_1 + P_1 A_1 - \rho_1^{-1} P_1 B_1 B_1^T P_1 + Q_1 = 0 . \tag{19}$$

Note that the friction team is not considered in the above control law. Thus, the feedforward team $\mu \operatorname{sgn}\left(\dot{x}_l\right)$ should be used to compensate for the friction. An optimal control law is given by:

$$u_1(t) = \rho_1^{-1} B_1^T P_1 E_1(t) + \mu \operatorname{sgn}(\dot{x}_m) . \tag{20}$$

From Eq. (1), Eq. (13), Eq. (20), we can get the desired torque of motor control:

$$T_{m1} = \frac{I}{2\pi\rho} (\rho_1^{-1} B_1^T P_1 E_1(t) + \mu \operatorname{sgn}(\dot{x}_m)) . \tag{21}$$

According to the parameter of Table.1 we can get:

$$A_1 = \begin{bmatrix} 0 & 1 \\ -0.69 & -0.2 \end{bmatrix}, \quad B_1 = \begin{bmatrix} 0 \\ 0.69 \end{bmatrix} . \tag{22}$$

The selection of the Q_1=diag{700,1}, ρ_1=1. Solving Eq. (19), Eq. (20) we can get:

$$P_1 = \begin{bmatrix} 228.9 & 36.9 \\ 36.9 & 12.1 \end{bmatrix}, \tag{23}$$

$$u_1(t) = 25.5e_1 + 8.4\dot{e}_1 + 42\,\mathrm{sgn}(\dot{x}_m). \tag{24}$$

The characteristic equation of the closed-loop system Eq. (18) can be written as:

$$s^2 + 174.3s + 1215 = 0. \tag{25}$$

Based on Routh criterion, this system is stable. From Eq. (21), the desired torque for motor control is given by:

$$T_{m1} = 12.8e_1 + 4.2\dot{e}_1 + 21\mathrm{sgn}(\dot{x}_m). \tag{26}$$

High force control

When NSSEA work in the high force range, the designed controller is similar to low operation force control. The force error is defined as $e_2 = F_{d2}(t) - F_{l2}(t)$, and the derivative force error is given by $\dot{e}_2 = \dot{F}_{d2}(t) - \dot{F}_{l2}(t)$ F_{d2}, refers to the desired force. Define the state matrix $E_2 = [e_2, \dot{e}_2]^T$, then the state equation can be written as:

$$\dot{E}_2 = \begin{bmatrix} \dot{e}_2 \\ \ddot{e}_2 \end{bmatrix} = A_2E_2 - B_2F_{m2} + B_2\left[\frac{m_m}{k_1+k_2}\ddot{F}_{d2} + \dot{F}_{d2} + \frac{b}{k_1+k_2}F_{d2} - \frac{m_m}{k_1+k_2}\Delta f(\dot{x}_m)\right], \tag{27}$$

where

$$A_2 = \begin{bmatrix} 0 & 1 \\ -\frac{k_1+k_2}{m_m} & -\frac{b}{m_m} \end{bmatrix},\quad B_2 = \begin{bmatrix} 0 \\ \frac{k_1+k_2}{m_m} \end{bmatrix}. \tag{28}$$

The control law can be written as:

$$u_2(t) = K_{p2}e_2 + K_{d2}\dot{e}_2, \tag{29}$$

where K_{p2}, K_{d2} are the appropriate gain parameters. Simplified the Eq. (27), we have the following linear model:

$$\dot{E}_2 = \begin{bmatrix} \dot{e}_2 \\ \ddot{e}_2 \end{bmatrix} = A_2E_2 - B_2F_{m2}, \tag{30}$$

$$F_{m2} = cu_2(t). \tag{31}$$

From Eq. (28)~(31), the linear model can be written as:

$$\dot{E}_2 = \begin{bmatrix} 0 & 1 \\ -\frac{k_1+k_2}{m_m} - \frac{c(k_1+k_2)}{m_m}K_{p2} & -\frac{b}{m_m} - \frac{c(k_1+k_2)}{m_m}K_{d2} \end{bmatrix} E_2. \tag{32}$$

Therefore, the characteristic equation of the closed-loop system is:

$$s^2 + \left(\frac{b}{m_m} + \frac{c(k_1+k_2)}{m_m}K_{d1}\right)s + \frac{k_1+k_2}{m_m} + \frac{c(k_1+k_2)}{m_m}K_{p1} = 0. \tag{33}$$

We apply the LQR design theory to optimize gain parameters. The performance index of optimal control is introduced, an input u_2 is designed to that:

$$J_2 = \int_0^\infty (E_2^T Q_2 E_2 + \rho_2 u_2{}^2)dt, \tag{34}$$

where Q_2 is a symmetric positive-definite matrix and refers to the weighting matrix for E_2, and ρ_2 is a positive constant. According to the LQR optimal control theory, if J_2 minimize, the feedback control law should be:

$$u_2(t) = \rho_2^{-1}B_2^T P_2 E_2(t), \tag{35}$$

where P_2 is a unique positive definite matrix and satisfies the famous Riccati differential equations:

$$A_2^T P_2 + P_2A_2 - \rho_2^{-1}P_2B_2B_2^T P_2 + Q_2 = 0. \tag{36}$$

We use feedforward team $\mu\,\mathrm{sgn}(\dot{x}_l)$ to compensate for the friction, an optimal control law is given by:

$$u_2(t) = \rho_2^{-1}B_2^T P_2 E_2(t) + \mu\,\mathrm{sgn}(\dot{x}_m). \tag{37}$$

Form Eq. (1), Eq. (31), Eq. (37), we can get the desired torque of motor control:

$$T_{m2} = \frac{I}{2\pi\rho}(\rho_2^{-1}B_2^T P_2 E_2(t) + \mu\,\mathrm{sgn}(\dot{x}_m)). \tag{38}$$

According to the parameter of Table.1 we can get:

$$A_2 = \begin{bmatrix} 0 & 1 \\ -6.4 & -2 \end{bmatrix}, B_2 = \begin{bmatrix} 0 \\ 6.4 \end{bmatrix}. \tag{39}$$

The selection of the Q_2=diag{700,1}, ρ_2=1. Solving Eq. (36), Eq. (37) we can get:

$$P_2 = \begin{bmatrix} 62 & 3.3 \\ 3.3 & 0.4 \end{bmatrix}, \tag{40}$$

$$u_2(t) = 21.4e_2 + 3.3\dot{e}_2 + 42\,\mathrm{sgn}(\dot{x}_m). \tag{41}$$

The characteristic equation of the closed-loop system Eq. (32) can be written as:

$$s^2 + 617.9s + 10204 = 0. \tag{42}$$

Based on Routh criterion, this system is stable. From Eq. (38), the desired torque for motor control is given by:

$$T_{m2} = 12.8e_2 + 4.2\dot{e}_2 + 21\mathrm{sgn}(\dot{x}_m). \tag{43}$$

Smooth switching control

Whether the NSSEA working form low force range to high force range or form high force range to low force range, the controller parameters should change accordingly. In the theory, switching control should be switched seamlessly at the switch point, and executed at the NSSEA. The NSSEA controller is naturally switched to the high force control when the desired force is greater than the maximum value of the low force range, and it is switched to low force control when the desired force is less than the minimum value of the high force range. However, due to the control error, the output force maybe shakes at the switch point. For example, when the desired force is increasing and close to the maximum value of the low force range, the output force maybe belongs to the high force range; or the desired force is decreasing and close to the minimum value of the high force range, the output force maybe belongs to the low force range. The all above case both will cause the mismatch of control law and the output force shaking. Fortunately, the two situations occur at the close the transition point. Therefore, smooth switching control is proposed in this paper. Near the transition point, a smoothing function is used to smooth the gain parameters. The controller parameters will not an abrupt change. The smoothing function is:

$$f_s(F_d, F_{L0}, F_{H0}) = \begin{cases} K_L & (F_d \le F_{L0}) \\ K_L + \frac{1}{2}\left(K_H - K_L\right)\left(1+\sin\left(\left(\frac{F_d - F_{L0}}{F_{H0} - F_{L0}} - \frac{1}{2}\right)\pi\right)\right) & (F_{L0} \le F_d \le F_{H0}) \\ K_H & (F_d \ge F_{H0}) \end{cases} \quad (44)$$

where F_{L0} and F_{H0} refer to the start-stop point of smooth operation. The selection of the start-stop point is F_{L0}=60N, F_{H0}=100N. K_L, K_H is the PD parameters of low force control and high force control.

EXPERIMENT

In this section, the designed control is applied to a prototype of the NSSEA. The experimental setup is shown in Fig.6. We press one end of the actuator with a pressure bar and fix the actuator on the experiment platform. The load end is fixed. To verify the effectiveness of the proposed control, a sinusoidal reference signal is used as the desired force, and the actuator is controlled to follow this force reference trajectory. In the controller, applied the STM32F407 as control chip. The sampling frequency of our experiment is 200Hz. We will evaluate the control performance at low force case, high force case and switching control case and all the data processed using Matlab 2016a.

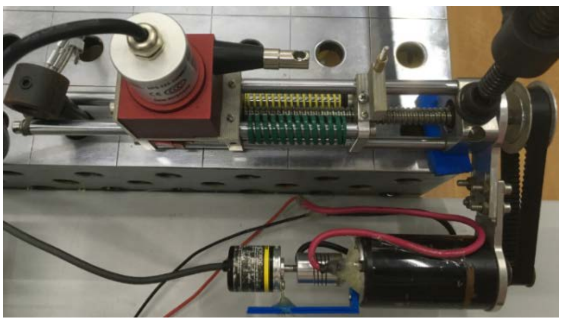

Figure 6. Experiment set-up.

Low force tracking control

Let us first consider the low force tracking control problem of the NSSEA. The low force is generated by the soft spring and the low force range is 0-75N. Eq. (26) is used as the control law. Fig.7 and Fig. 8 shows the tracking control results. Fig. 7(a) shows the trajectory tracking the performance of the NSSEA when 2 Hz sinusoidal reference used as the desired force. Fig. 7(b) shows the tracking error at a frequency of 2 Hz. It is clear from the figure that the maximum tracking error is very small that is 1.7N. To quantify the corresponding fidelity, a measured was defined based on the variance-accounted-for factor:

$$fidelity = \left(1 - \frac{\mathrm{var}(y-R)}{\mathrm{var}(y)}\right)100\%, \quad (45)$$

where y is the vector of the sampled measurement and R refers to the vector of the sampled sine. According to the definition, the force fidelity is 99.7% at the frequency of 2 Hz. Fig. 8(a) shows the trajectory tracking performance of the NSSEA when 4 Hz sinusoidal reference input is applied. Fig. 8 (b) shows the tracking error at a frequency of 4 Hz. The results show that the maximum tracking error about 3.7N. The value of the force fidelity is 98.6% at the frequency of 4 Hz. It is clear from the experimental results that the proposed control provides high-performance trajectory tracking control.

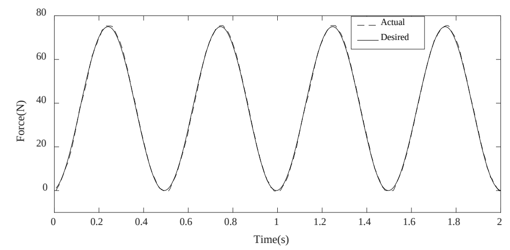

(a) Sinusoidal trajectory tracking with a frequency of 2 Hz

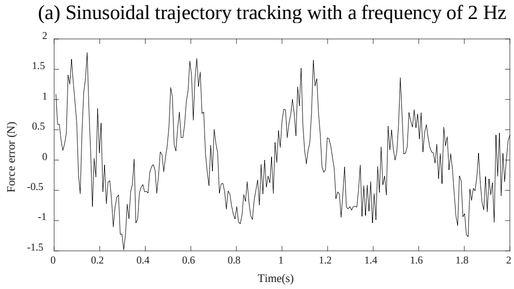

(b) Force error at the frequency of 2 Hz

Figure 7. Tracking control performance of low force range for 2 Hz.

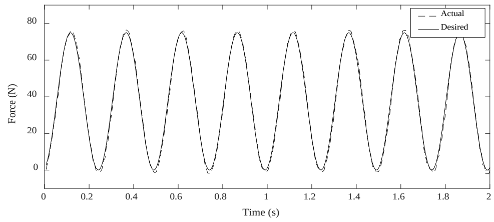

(a) Sinusoidal trajectory tracking with a frequency of 4 Hz

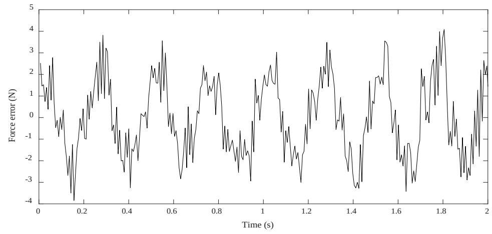

(b) Force error at the frequency of 4 Hz

Figure 8. Tracking control performance of low force range for 4 Hz.

High force tracking control

The high force is generated by the parallel connection of soft and stiff spring and the high force range is 75-150N. Eq. (43) is used as the control law at high force case. Fig. 9 and Fig. 10 shows the tracking control results. In particularly, Fig. 9(a) shows the trajectory tracking the performance of the NSSEA when 2 Hz sinusoidal reference used as the desired force. Fig. 9(b) shows the tracking error at a frequency of 2 Hz. The result shows that the maximum tracking error is 4N. The force fidelity is 96.7%. Fig. 10(a) shows the trajectory tracking performance of the NSSEA when 4 Hz sinusoidal reference input is applied. Fig. 10(b) shows the tracking error at a frequency of 4 Hz. It is clear from the figure that the maximum tracking error about 8.5N. The value of the force fidelity is 93.3% at the frequency of 4 Hz.

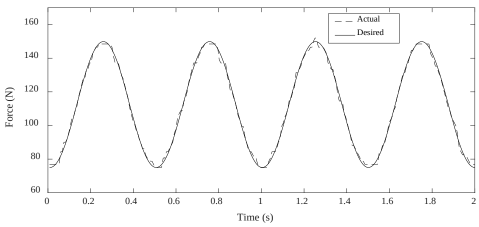

(a) Sinusoidal trajectory tracking with a frequency of 2 Hz

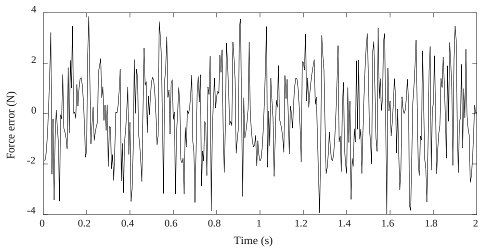

(b) Force error at the frequency of 2 Hz

Figure 9. Tracking control performance of High force range for 4 Hz.

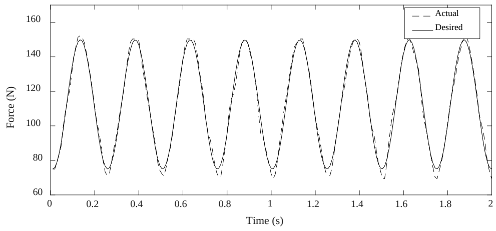

(a) Sinusoidal trajectory tracking with a frequency of 4 Hz

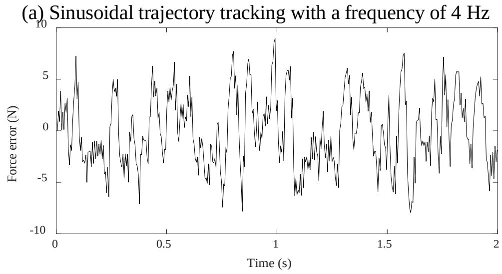

(b) Force error at the frequency of 4 Hz

Figure 10. Tracking control performance of High force range for 4 Hz.

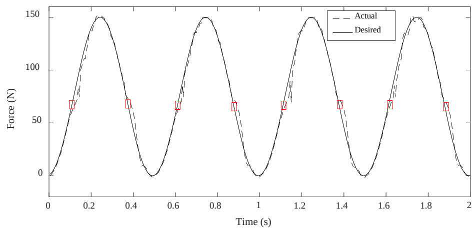

(a) Sinusoidal trajectory tracking with a frequency of 2 Hz

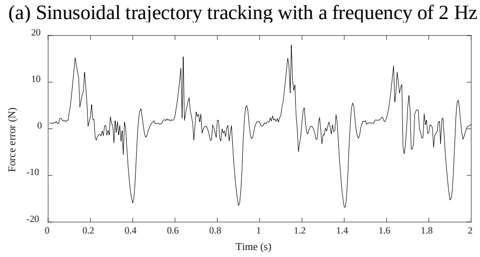

(b) Force error at the frequency of 2 Hz

Figure 11. Tracking control performance of wide-bound force range for 2 Hz.

Wide-bound force tracking control

In practical application, the NSSEA works in both low and high force ranges. In this case, the smooth switching control is used at the closing of the transition point. It is important to estimate the start-stop point of smooth operation. Within the set of switching ranges, the parameters of the proposed controller are smoothed according to Eq. (44). Fig. 11 and Fig. 12 shows the force tracking control results. Fig. 11(a) shows the trajectory tracking the performance of the NSSEA when 2 Hz sinusoidal reference used as the desired force, and the rectangle mark is the transition point. Fig. 11(b) shows the tracking error at a frequency of 2 Hz. The result shows that the maximum tracking error about 17N. The force fidelity is 93.5%. Fig. 12(a) shows the trajectory tracking performance of the NSSEA when 4 Hz sinusoidal reference input is applied. Fig. 12(b) shows the tracking error at a frequency of 4 Hz. It is clear from the figure that the maximum tracking error about 20N. The value of the force fidelity is 91.6% at the frequency of 4 Hz.

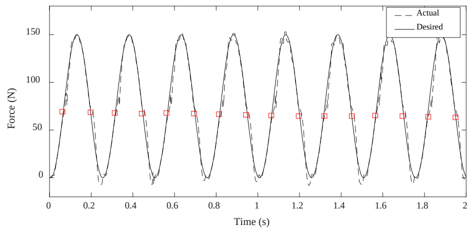

(a) Sinusoidal trajectory tracking with a frequency of 4 Hz

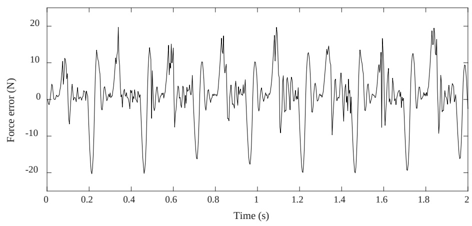

(b) Force error at the frequency of 4 Hz

Figure 12. Tracking control performance of wide-bound force range for 4 Hz.

DISCUSSION

Using the proposed controller, the novel SEA can track the sinusoidal trajectory with a frequency of 4 Hz. When NSSEA work in the low force range, the maximum tracking error is very small, about 1.7N at the frequency of 2 Hz and 3.7N at the frequency of 4 Hz, and the value of force fidelity is 99.7% and 98.6% individually. By contrast, for the high force range, the maximum tracking error is larger about 4N at the frequency of 2 Hz and 8.5N at the frequency of 4 Hz, and the value of force fidelity is 96.7% and 93.3% individually. This is due to the course accuracy of spring compression measurement which is 0.1mm, the corresponding force accuracy is 6.8N. Improving the accuracy of spring compression measurement is an effective way to reduce the tracking error. When NSSEA work at wide-bound force case, the maximum tracking error appears at the near transition point, about 17N at the frequency of 2 Hz and 20N at the frequency of 4 Hz, and the value of force fidelity is 93.5% and 91.6% individually. It can be seen that although the controller switches between low and high forces ranges, the system is still stable with the cost of slightly larger tracking error at the near transition point. This is because a compromise smoothing control parameter is adopted to avoid output force oscillation near the transition point. Considering the wide-bound force range, the result is acceptable.

CONCLUSION

In this paper, a novel two different series elastic actuator is proposed for overcoming the limitation due to the compromise on the elastic element stiffness selection and designed a segmental model-based feedback controller and smooth switching controller for the actuator. The novelty of the NSSEA design is used soft and stiff springs parallel as the elastic element of the actuator. The low stiffness linear spring worked at low force range and the parallel connection of two linear spring is operated at the high force range. The experimental results based on the NSSEA prototype have demonstrated that the proposed controller can achieve excellent force tracking performance at both low, high, and wide-bound force range. In the next stage, we will continue to research the performance of the NSSEA and test to apply it to human-centered robotics.

ACKNOWLEDGEMENT

This work was supported by “the Fundamental Research Funds for the Central Universities” [2018-JL-003] and National Natural Science Foundation of China under Grant [61603284].

REFERENCES

Boccanfuso, L., Scarborough, S., Abramson, R. K., Hall, A. V., and Jason M. O’Kane. “A low-cost socially assistive robot and robot-assisted intervention for children with autism spectrum disorder: field trials and lessons learned.” Autonomous Robots Vol. 41, pp. 637-655 (2017).

Kui X., Chang, Y., Kaiyang, Y., and Yunjian, G. “An ankle exoskeleton for walking assist.” Journal of Huazhong University of Science and Technology (Natural Science Edition), Vol. 43, pp.367-371 (2015).

Tadele, T. S., De Vries, T., and Stramigioli, S. “The safety of domestic robotics: A survey of various safety-related publications.” IEEE robotics & automation magazine, Vol. 21, Issue. 3, pp. 134-142 (2014).

Pratt, G, A., and Williamson, M, M., “Series Elastic Actuators.” Proc.ieee Int.conf.on Intelligent Robots & Systems, pp. 399-406 (1995).

Orekhov, Viktor, L., and Knabe, C, S. “An unlumped model for linear series elastic actuators with ball screw drives.” 2015 IEEE/RSJ International Conference on Intelligent Robots and Systems (IROS). IEEE, (2015).

Baldoni, A., Cempini, M., Cortese, M., Crea, S., Carrozza, M, C., and Vitiello, N., “Design and validation of a miniaturized SEA transmission system." Mechatronics Vol. 49, pp. 149-156 (2018).

Roozing, W., Malzahn, J., Kashiri, N., Caldwell, D. G., and Tsagarakis, N. G. "On the stiffness selection for torque-controlled series-elastic actuators." IEEE Robotics and Automation Letters. Vo. 2.4, Issue.4, pp. 2255-2262 (2017).

Wolf, S., Grioli, G., Friedl, W., Grebenstein, M., and Vanderborght, B. "Variable stiffness actuators: Review on design and components." IEEE/ASME transactions on mechatronics Vol. 21, Issue. 5, pp. 2418-2430 (2016).

Li-Ming, S., Zu-Wen, W., and Gang, B. "A comparison of mechanical properties of pneumatic muscle with biological muscle". Machine Tool & Hydraulics, Vol. 36, Issue. 6, pp. 22-24 (2004).

Paine, N, Sehoon Oh, and Luis S. "Design and control considerations for high-performance series elastic actuators." IEEE/ASME Transactions on Mechatronics Vol. 19, Issue. 3, pp. 1080-1091, (2014).

Yin, K., Pang, M., Xiang, K., and Chen, J. "Optimization Parameters of PID Controller for Powered Ankle-foot Prosthesis Based on CMA Evolution Strategy." 2018 IEEE 7th Data Driven Control and Learning Systems Conference (DDCLS). IEEE, (2018).

Roozing, W., Malzahn, J., Caldwell, DG., Tsagarakis, NG. "Comparison of open-loop and closed-loop disturbance observers for series elastic actuators." 2016 IEEE/RSJ International Conference on Intelligent Robots and Systems (IROS). IEEE, (2016).

Vallery, H., Veneman, J., Asseldonk, E., Ekkelenkamp, R., Buss, M., and Kooij, H. "Compliant actuation of rehabilitation robots." IEEE Robotics & Automation Magazine. Vol. 15, Issue. 3, pp. 60-69 (2008).

Kong, K., Bae, J., and Tomizuka, M. "Control of rotary series elastic actuator for ideal force-mode actuation in human–robot interaction applications." IEEE/ASME Transactions on Mechatronics. Vol. 14, Issue. 1, pp. 105-118 2009.

Yin, K., Pang, M., Xiang, K, Chen, J., and Zhou, S. "Fuzzy iterative learning control strategy for powered ankle prosthesis". International Journal of Intelligent Robotics and Applications, Vol. 2, Issue. 1, pp. 122-131 (2018).

Kwakernaak, H., and Sivan, R. "Linear optimal control systems." Wiley-interscience. (1972).

NOMENCLATURE

m_m Equivalent mass of the motor
b_m Damping of motor and ball screw
F_{max} Max output force
k_1 Low stiffness spring constant
k_2 Larger stiffness spring constant
l_1 Alone working stroke of soft
l_2 Both spring parallel working
L Length of the ball screw
I Pitch of the ball screw
M Total weight of the actuator
F_m Motor equal input force
F_{m1} Motor equal input force in the low force range
F_{m2} Motor equal input force in the high force range
F_{l1} Output force in the low force range
F_{l2} Output force in the large force range
T_r Motor input torque
x_m Ball screw nut relative position
J_1 Motor inertia moment
μ Frictional force parameter
Δx Displacement of the spring contraction
F_{d1} Desired output force in the low force range
F_{d2} Desired output force in the large force range
e_1 Force error in the low force range
e_2 Force error in the large force range
E_1 Force error state matrix in the low force range
E_2 Force error state matrix in the high force range
K_{p1} Proportional parameter in the low force range
K_{d1} Derivative parameter in the low force range
K_{p2} Proportional parameter in the high force range
K_{d2} Derivative parameter in the large force range
T_{m1} Torque Control command low force range
T_{m2} Torque Control command high force range
c Motor torque constant

新型雙剛度串聯彈性驅動器的設計與控制

尹凱陽 向馗 陳靜 龐牧野
武漢理工大學自動化學院
平頂山學院電氣與機械工程學院

摘要

串聯彈性驅動器被廣泛應用於人機協作機器人，傳統串聯彈性驅動器面臨著由於彈性器件的折中選擇引起的性能限制。本文提出一種新型的雙剛度串聯彈性驅動器並設計配套優化控制演算法，以解決這一性能限制。主要表現為，兩個剛度與長度都不相同的線性彈簧並聯作為彈性器件。在低作用力輸出範圍內，剛度小的彈簧其作用，而在高作用力範圍內，兩個彈簧共同作用。設計一種平滑控制器用於解決在高低作用力區間的平滑切換的問題。實驗結果表明，提出雙剛度串聯彈性驅動器在低作用力區間、高作用力區間、和同時包含高低作用力區間都能達到滿意的力輸出跟蹤性能。